Hydrothermal Alteration in the New Deep Geothermal Well GIL-1 (Strasbourg Area, France)

Carole Glaas, Patricia Patrier, Jeanne Vidal, Daniel Beaufort, Jean-François Girard, Albert Genter

Proceedings World Geothermal Congress 2020
Reykjavik, Iceland, April 26 – May 2, 2020

Hydrothermal Alteration in the New Deep Geothermal Well GIL-1 (Strasbourg Area, France)

Carole Glaas[1,2], Patricia Patrier[3], Jeanne Vidal[1,4], Daniel Beaufort[3], Jean-François Girard[2], Albert Genter[1]

[1]ES-Géothermie, Bat Le Belem 5 rue de Lisbonne, 67300 Schiltigheim, France, [2]University of Strasbourg, CNRS, UMR 7516 IPGS, 5 Rue René Descartes, 67084 Strasbourg Cedex, France, [3]University of Poitiers, CNRS UMR 7285 IC2MP, HydrASA, Bat B8 rue Albert Turpain, TSA51106, F-86073 Poitiers Cedex 9, France, [4]University of Chile, FCFM, Dept. of Geology, Andean Geothermal Center of Excellence (CEGA), Plaza Ercilla 803, Santiago, Chile

carole.glaas@es.fr

Keywords: illite, clay minerals, fracture zone, granitic reservoir, X-ray diffraction (XRD), Short Wave Infrared (SWIR), Illkirch, Upper Rhine Graben (URG)

ABSTRACT

The first geothermal well of Illkirch located South of Strasbourg (France), GIL-1, has been drilled to 3.8 km deep in a granitic basement. Drill cuttings and geophysical logs from basement were investigated in terms of hydrothermal alteration and natural fractures respectively. Petrographic observations of the 250 cuttings samples between 2900 and 3800 m MD were conducted on-site during the drilling with binocular loupe and enabled to identify the hydrothermal alteration grades in the open-hole granitic section of the well. From binocular examination, secondary minerals like drusy quartz, carbonates and anhydrite were spatially correlated to the occurrences of natural fractures. In the granitic section corresponding to propylitic alteration, phyllosilicates include primary biotite, muscovite and secondary chlorite. Then, 48 cuttings samples were analyzed by X-ray diffraction (XRD) to identify the secondary clay mineralogy corresponding to poorly crystallized illite (PCI) and illite-rich illite-smectite mixed layers (I/S ML) which generally takes place within fractured zones (FZs). Mud logging and geophysical logs acquired in the granitic section of GIL-1 well have been used for characterizing fracture location (calcimetry, temperature log) and fracture orientation (electrical image logs). The granitic section of the well is characterized by a dense network of natural fractures. From 2900 to 3300 m MD, about 220 electrical conductive fractures have been observed on the image logs. From temperature logs, three main permeable zones have been identified and correlated with the occurrences of natural conductive fractures. From 2900 to 3200 m MD, the clay signature is mainly governed by the occurrences of PCI and I/S ML which are correlated to permeable FZs. In the deepest part of the granitic section, secondary chlorite and possible secondary well crystallized illite (WCI) have been observed. In parallel, an innovative short-wave infrared (SWIR) spectroscopy method was developed for characterization of clay minerals in those fractured reservoirs. It was first applied to the granitic section of the Soultz and Rittershoffen geothermal wells (Alsace, France). This time-saving method allows the quantification of illitic hydrothermal alteration and indirectly the recognition of permeable FZs. In perspective, SWIR data acquired in GIL-1 will also be analyzed in order to confirm the applicability of this routine and cheap method for deep geothermal well in the Upper Rhine Graben (URG).

1. INTRODUCTION

Since more than 30 years, a geothermal rush was observed in the Upper Rhine Graben (URG). The pioneer project of Soultz-sous-Forêts investigated the naturally fractured granitic reservoir within four geothermal deep wells (5 km). The nearby Rittershoffen project took then advantage of the lessons learned from Soultz by drilling two deep geothermal wells (3km) in the granitic basement targeting the multiscale network of fractures. Two more geothermal projects are under drilling operations in the Strasbourg area, in Vendenheim and in Illkirch. This contribution focuses on the preliminary geological results (petrography, secondary mineralogy, natural fractures) collected in the granitic section of the Illkirch GIL-1 well drilled to 3.8 km. The mid-Carboniferous granitic basement of the URG has been affected by several extensional and compressional tectonic phases which developed a multi-scale fracture network (Schumacher, 2002; Villemin and Bergerat, 1987). In deep geothermal projects, the target is to cross these natural fracture zones (FZs) which are today the seat of hydrothermal circulations and act as the main pathways for the natural brine through wide convection cells (Baillieux et al., 2013; Dezayes and Lerouge, 2019; Schellschmidt and Clauser, 1996). At the top of the highly fractured granitic basement, several temperature anomalies localized along the main faults are the expression of the fluid circulation in the FZs (Figure 1). In these complex FZs, specific mineralogical assemblages are evidences of paleo or present hydrothermal circulations. Clay minerals like illite, chlorite and tosudite are very sensitive to the fluid/rock (F/R) ratio, to the pH and to the temperature and are systematically precipitated in FZs (Ledésert et al., 2010). But the occurrence of other secondary minerals like drusy quartz, carbonates, barite, and anhydrite is also associated to fracture infillings (Smith et al., 1998; Traineau et al., 1992). Hence, this study will investigate the alteration mineralogy in the granitic section of the deviated GIL-1 well drilled between 2.9 and 3.8 km. Alteration mineralogy from about 250 cuttings will be derived from petrographic observation with binocular loupe and with X-ray diffraction (XRD). These petrographic results will be linked to the FZs occurrences on the electrical image logs. The goal will be to identify the clay signature of FZs in the granitic basement. These preliminary results aim to calibrate the short-wave infrared (SWIR) data acquired in the GIL-1 well. This innovative SWIR method already demonstrated its applicability to the granitic basement of the URG with the Soultz and Rittershoffen case studies whose examples will also be presented (Glaas et al., 2019; Vidal et al., 2018a).

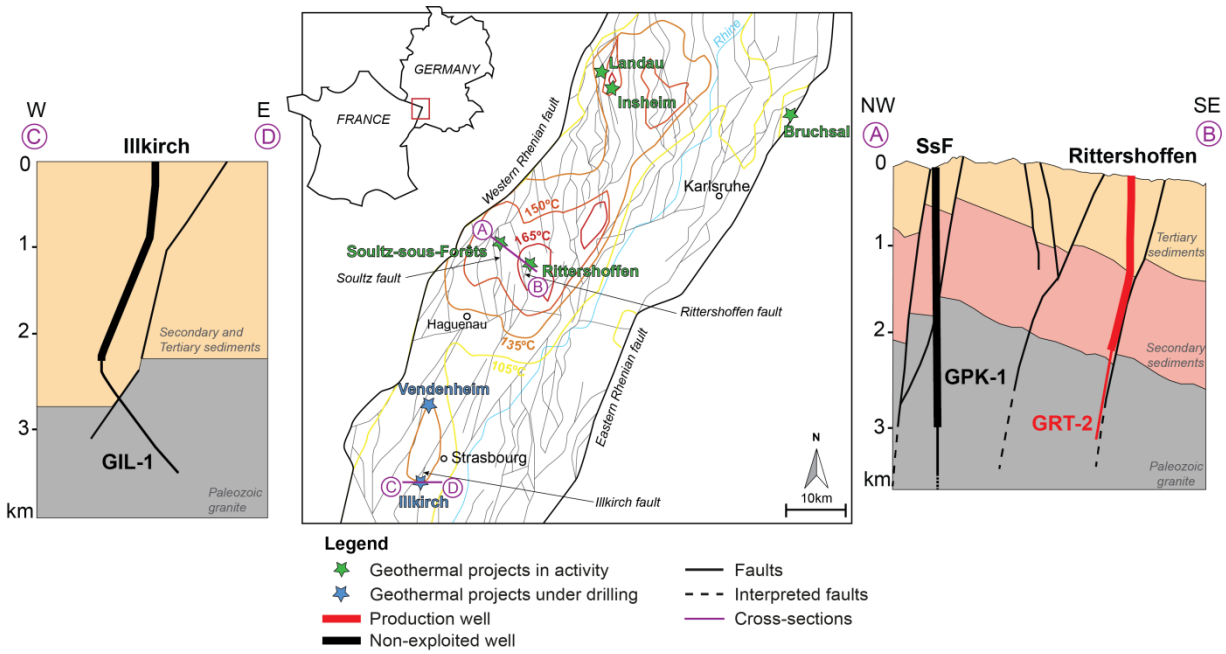

Figure 1: Structural map of the center of the Upper Rhine Graben with isotherms at 2 km depth after Vidal et al., (2019) and the geoportal GeOrg (GeOrg, 2017). The geothermal anomaly in the Strasbourg area is from the dataset of Baillieux et al., (2013). On the left: W-E cross section through the geothermal well of the Illkirch geothermal well with a simplified geology. On the right: NW-SE cross-section through the geothermal wells of Soultz and Rittershoffen. The thick line represents the casing section of the well, whereas the thin one represents the open hole.

2. GEOLOGICAL SETTING

2.1 The fractured and altered granitic basement in the URG

All the deep wells drilled into the granitic basement of Soultz and Rittershoffen provide a wide knowledge of the multiscale fracture network intersected (Dezayes et al., 2010; Genter and Traineau, 1996; Sausse and Genter, 2005). Core samples available at Soultz show small-scale fractures with no evidence of displacement, filled by carbonates, chlorite, iron oxides, epidote and sulphides. Intersections of faults were also observed with a filling of drusy quartz, carbonates, barite and clay minerals. Nowadays, in the URG, the target for geothermal projects is the permeable FZs lying in the first hundred meters of the hydrothermally altered granitic reservoir (Vidal and Genter, 2018). Investigation of the alteration parageneses could be a good indicator of the paleo and present-day circulations in the well and thus, of the localization of the permeable FZs intersected. During the cooling of the crystalline pluton, the granite underwent a pervasive alteration which presents the petrographic and mineralogical features of the propylitic facies. Today, it exhibits several grades of hydrothermal alteration related to fluid circulation in natural fractures (Ledésert et al., 2010; Traineau et al., 1992). The unaltered crystalline granitic basement at Rittershoffen and Soultz-sous-Forêts geothermal sites (located tens of kms North of Strasbourg) is composed of primary muscovite, biotite, K-feldspar, plagioclase, and quartz (Stussi et al., 2002; Traineau et al., 1992). This primary mineralogy is affected by hydrothermal alteration, and specific mineralogical associations are reflecting the several alteration grades encountered. According to the previous studies on the Soultz-sous-Forêts geothermal wells, the hydrothermal alteration grades in the granite are well known from core observations (Ledésert et al., 1999; Meller et al., 2014; Meller and Kohl, 2014; Meller and Ledésert, 2017; Sausse et al., 2006; Traineau et al., 1992). The core mineralogy and hydrothermal alteration grades were then cross-referenced with the minerals observed in the cuttings at Rittershoffen, although the texture information and the mineral assemblage were not reflected in the cuttings (Figure 2). The low hydrothermal alteration (HLOW) grade is characterized by more chlorite than primary biotite, the absence or minor amount of secondary illite, and unaltered primary plagioclase and K-feldspars. The moderate hydrothermal alteration (HMOD) grade is characterized by the presence of illite due to the further alteration of chlorite, plagioclase and K-feldspar (weakly altered); fresh and weakly altered biotite is observed in minor amounts. The high hydrothermal alteration (HHIG) grade is associated with abundant illitic material, very low amounts of chlorite, strongly altered plagioclase and K-feldspar, and relics of altered biotite. The extreme hydrothermal alteration (HEXT) grade is characterized by the total depletion of biotite, abundant illitic material replacing primary biotite, plagioclase and K-feldspar, as well as drusy quartz prisms linked to hydrothermal circulation (Genter et al., 1997; Nishimoto and Yoshida, 2010; Traineau et al., 1992). The VEIN facies defines the core of the fracture zone identified by the highest amounts of secondary drusy quartz and its association with a high calcite content (Hébert et al., 2010; Ledésert et al., 2009). The granitic facies identified in the cuttings include an “unaltered” granite (GRAN), which is characterized by the presence of biotite, hematite, calcite, and affected by a propylitic alteration related to the cooling of the pluton (Genter et al., 2000; Jacquemont, 2002), and locally reddish granite (RED), which contains a large amount of red K-feldspar megacrysts oxidized through intense exposure to weathering fluids. In Soultz and Illkirch the GRAN shows facies variations with high amounts of muscovite named two-mica granite (GR2M) (Cocherie et al., 2004). The presence of illite in the granitic basement as a major signature of hydrothermal alteration was also confirmed by complementary laboratory analyses. In previous studies on the Rittershoffen wells, (XRD) was performed on the <5 µm fraction of selected cuttings, from which three groups of illitic minerals (well-crystallized illite (WCI), poorly crystallized illite (PCI), and illite-rich illite/smectite mixed layers (I/S ML)) were identified (Vidal et al., 2018b). The chemical compositions of the clay minerals were obtained using a scanning electron microscope (SEM) coupled with energy-dispersive X-ray spectroscopy (EDS). This study showed that permeable FZs were associated with the occurrence of poorly PCI

and I/S ML crystallized during hydrothermal circulation (Vidal et al., 2018b). XRD measurements in the Soultz wells also evidenced the presence of illite in fractured and altered zones as well as the presence of chlorite and biotite in HLOW and GRAN.

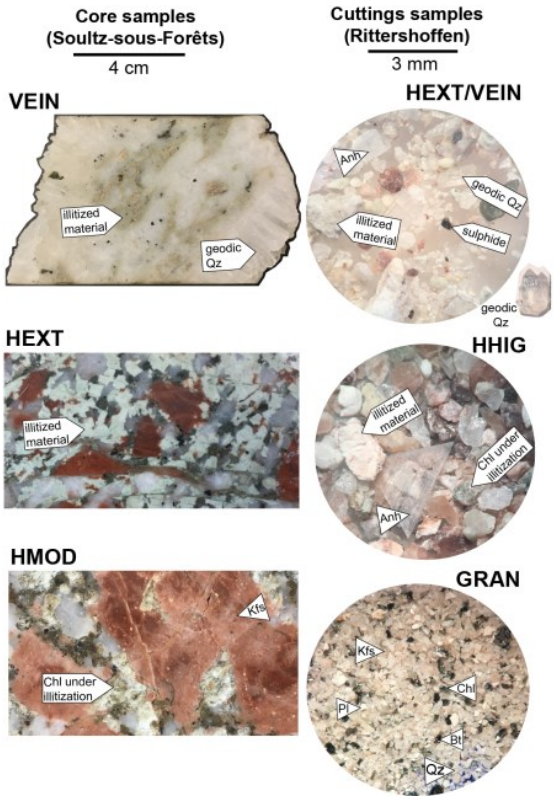

Figure 2: Examples of mineralogical assemblages of the granitic basement observed in cores (left) and observed in cuttings (right), defining the several hydrothermal alteration grades from Glaas et al., (2019).GRAN: unaltered granite, HMOD: moderately hydrothermally altered granite, HHIG: highly hydrothermally altered granite, HEXT: extremely hydrothermally altered granite, VEIN: secondary drusy quartz vein.

2.2 Illkirch site

The main objective of this geothermal project is to generate electricity and to supply yearly about 50 GWh of heat to a neighboring district heating network in the suburb of Strasbourg. Exploration works were carried out between 2013 and 2016: gravimetric surveys, aeromagnetic survey, reprocessing of vintage 2D seismic data, new 2D seismic data acquisition (35k m in 2015) and all available data, including numerous oil and geothermal exploration well data, which could be integrated to get a detailed picture of the deep underground around the project's location (Edel et al., 2018; Richard et al., 2016). The defined geothermal target was a major fault zone with a normal off-set of 800 m located at the interface between sedimentary cover (clastic Triassic sandstone) and crystalline basement (Figure 1). Expected temperature is 150°C with a nominal flow rate of 70 l/s. The drilling of the first deviated well GIL-1 ended in July 2019 at the total depth of 3.8 km. The GIL-1 well reached the top basement at 2.9 km which corresponds to the target fault zone oriented N20°E and dipping, 70°W from electrical image logs.

3. MATERIALS AND METHODS

3.1 Materials

The cuttings (chip samples) collected during the drilling of the wells are first washed and then dried on-site. Depending on the well section and on the sampling distance of the cuttings, the sample will represent a variable volume of rock (Table 1). The average size of the cutting grains varies between 0.5 and 2 mm in each sample. This cuttings grain size can be highly influenced by the drilling tool wearing and thus could influence the SWIR absorption feature.

Table 1: various rock volumes represented by the cuttings samples for different sections of the GIL-1 well.

well	section	depth interval	sampling distance	volume of rock
GIL-1	8"1/2	2894-3324mMD	5m	160L
	6"	3324-2694mMD	5m	90L

3.2 Methods

This petrographic study is based on a multi-approach methodology correlating datasets with different scales from sample to drill hole scale and various techniques (Figure 3). This methodology is about to be applied to the GIL-1 well, where the binocular loupe observations and XRD analyses were already performed. Electrical image logs were also acquired and this study will focus on the first part of the methodology presented in the Figure 3 by correlating the results from these methods before interpreting the SWIR results.

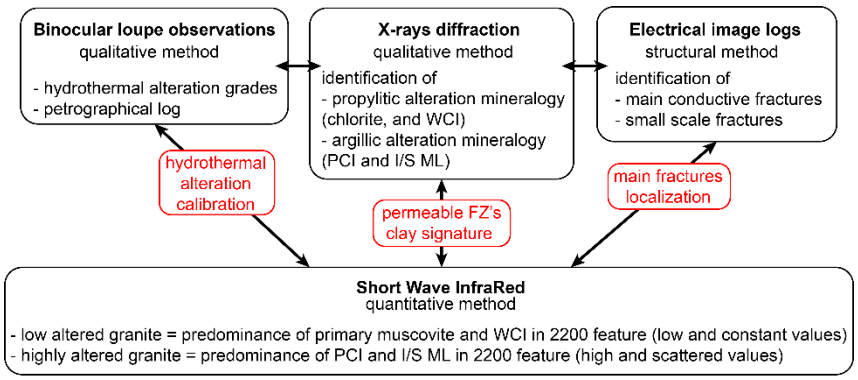

Figure 3: Workflow used for characterizing hydrothermal mineralogy in the granitic basement of URG geothermal wells. Abbreviations: well crystallized illite (WCI), poor crystallized illite (PCI), illite-smectite mixed layers (I/S ML).

3.2.1 X-ray diffraction method

XRD was made on selected cuttings samples of the GIL-1 well to identify clay minerals. In total, 48 cuttings samples were collected from the GIL-1 well. The sampling was concentrated in the permeable and altered FZs but also in the GRAN and GR2M which serve as reference materials as it is believed to be representative of rocks preserved from actual fluid circulation properties. 15 samples were prepared as disoriented powders of the bulk rock to analyze the whole rock mineralogy. The cuttings were grinded using a ring and agate mills. Analyses were carried out on a Phillips diffractometer (CuKα radiation, 40kV, 40mA). The analytical conditions were as follow: angular domain: 2-65° 2θ; step increment: 0.0235 2θ and counting time per step: 0.90 s. Then, 48 samples including the 15 samples that were analyzed for bulk rock mineralogy were dispersed in distilled water by ultrasonic vibration without any preliminary grinding to avoid contamination of the <5µm fraction by primary micas. Oriented powders were prepared from the <5µm fraction size separated from suspension in water by sedimentation. Clay minerals were identified by XRD of air-dried (AD) and ethylene-glycol (EG)-saturated oriented powders carried out on a Phillips diffractometer (CuKα radiation, 40kV, 40mA). The analytical conditions were as follow: angular domain: 2-35° 2θ; step increment: 0.0235 2θ and counting time per step: 0.73 s. XRD data acquisition and treatment were conducted using the X'Pert HighScore software (PANalytical B.V.). The clay minerals were identified according to the literature (Brindley and Brown, 1980; Moore and Reynolds, 1997). In this study, we measure the full width at half maximum (FWHM) and intensities of the 7 Å and 10 Å reflections as well as the ratio between the intensity of the d_{002} and the d_{001} reflections (noted I_{002}/I_{001}) on the oriented powders diffractograms. The 10 Å reflection observed on the diffractogramms is in our study the integration of the intensities diffracted by the micas and illitic minerals (illite and illite-rich I/S ML). However, it is possible to identify the dominant phyllosilicate from the following parameters.

- The ratio I_{002}/I_{001} is lower than 0,10 for trioctahedral micas (biotite), whether dioctahedral clays (muscovite and illite) will have a ratio between 0,37 and 0,55.

- The FWHM of the 10 Å reflection enables to differentiate the contribution between muscovite and illite: higher the FWHM, lower the crystallinity along the c axis. The muscovite presents a FWHM lower than the one of illite (Figure 4).

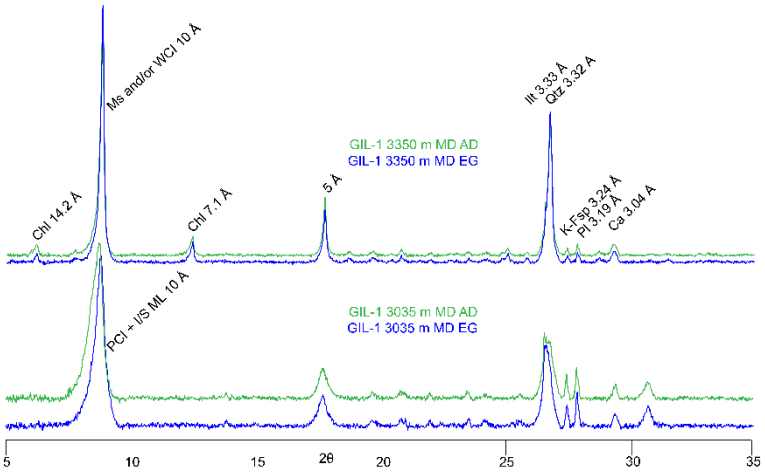

Figure 4: XRD results in the GIL-1 well of oriented samples of the fraction <5 µm from GIL-1. Comparison between air dried (AD) and ethylene-glycol (EG) conditions. The sample at 3035 m MD presents a predominance of illite-rich illite-smectite mixed layers (I/S ML) and poor crystallized illite (PCI) whereas the sample at 3350 m MD presents a predominance of muscovite and/or well crystallized illite (WCI).

3.2.2 Temperature anomalies

Temperature (T) anomalies are interpreted as the signature of circulations between the well and the formation (Barton et al., 1995; Bradford et al., 2013; Davatzes and Hickman, 2005; Vidal et al., 2019). In the case of T profiles acquired at equilibrium and comporting negative and positive T anomalies, positive anomalies are interpreted as open FZs where hotter brine than the formation

circulates, whereas negative anomalies are interpreted as open FZs where colder water than the formation circulates (Vidal et al., 2019). In the GIL-1 well, the T profiles were not acquired at equilibrium but 12 hours after injection. This implies that the open FZs are cooled by the injected fluid inducing only negative T anomalies. Thus, in the GIL-1 well, only the localized depth sections of the T anomalies were represented in the Figure 5, showing in blue sections the occurrence of T anomalies.

3.2.3 Electrical image logs

Image logs have been intensively used in the Soultz and Rittershoffen wells mainly with acoustic logs (Genter et al., 1995; Vidal et al., 2019). The open-hole section of the GIL-1 well was completely imaged by electrical image logs. Composed of 8 pads the electrical imager tool measures the resistivity of the borehole wall providing an unwrapped image of the borehole wall. On this unwrapped image, sinusoids are the trace of natural conductive fractures. A low conductivity is expressed by light colours (yellow to white) whereas a high conductivity is expressed by darkest colours (black). In the data presented in this study (Figure 6), the static image on the left is normalized over the complete depth interval of the well and thus the contrast responds to large-scale variations in lithology, porosity and saturation whereas the dynamic image on the right is normalized using a sliding window of 0.5 m; this highlights small-scale variations in contrast due to bedding, fractures, and changes in porosity. In the Figure 5 and Figure 6, very conductive fractures (appearing black on both dynamic and static images) were reported in red dots along depth. As both the very saline brine and the clay minerals are very conductive, a black fracture on both static and dynamic images could even be interpreted as an open fracture with very saline and conductive brine, or as a clogged fracture filled by conductive secondary clay minerals.

4. RESULTS: HYDROTHERMAL ALTERATION FACIES AND PERMEABLE FZS IN GIL-1

4.1. Petrographical log from binocular loupe observations

The petrographical log of the granitic section of the GIL-1 well is composed of three main zones:

- **2900-3100 m MD**. The first zone, highly altered and fractured, is observed at the top of the granitic basement from 2900 to 3100 m MD (Figure 5). The binocular observations revealed the absence of primary biotite, the presence of illitic material identified by the dusty aspect of the cuttings samples, as well as the occurrence of hematite and small amounts of calcite. Locally, hydrothermal drusy quartz was also observed in this zone at 3012 and 3022 m MD and anhydrite from 3050 to 3100 m MD (Figure 5).
- **3100-3350 m MD**. The second zone, fractured but less altered, is then observed from 3100 to 3350 m MD where primary biotite was commonly observed. The top of this zone from 3100 to 3200 m MD revealed the presence of hydrothermal drusy quartz, anhydrite and hematite, yielding a moderate hydrothermal alteration (HMOD). A small section of low hydrothermally altered granite described as a two-mica granite rich in muscovite is present from 3200 to 3220 m MD (Figure 5).
- **>3350 m MD**. The third zone, from 3350 to 3703 m MD is characterized by low hydrothermal alteration grades and the presence of unaltered two-mica granite clearly visible from 3357 to 3445 m MD and at the bottom from 3683 to 3703 m MD. Biotite, muscovite and chlorite were regularly observed in considerable amounts in these sections. On the contrary, between 3500 and 3650 m MD moderate to high hydrothermal alteration are associated with drusy quartz as well as anhydrite and hematite.

4.2 XRD results

The first zone from 2900 to 3100 m MD where illitic material was identified from binocular loupe observations is characterized by the predominance of illite and illite-rich I/S ML. Illite is characterized by the reflections at 10, 5 and 3.33 Å in AD and EG without any shift. Illite-rich I/S ML differ from illite by presenting a slight change of the profile after EG saturation (light blue dots in the Figure 5). FWHM of d_{001} reflection at 10 Å is scattered between 0.25 and 0.6 °2θ.

The second zone from 3100 to 3350 m MD is characterized by the predominance of micas and/or WCI. The FWHM of d_{001} reflection at 10 Å varies between 0.15 and 0.3 °2θ. The ratio I_{002}/I_{001} of the lower FWHM 10 Å reflections suggests the predominance of biotite (in the <5µm fraction). Its occurrence in the fine fraction can be due to its partial destabilization into chlorite. The d_{060} at 1.49 Å observed on the disoriented pattern evidences also the occurrence of muscovite in these samples.

The third zone from 3350 to 3700 m MD is quite heterogeneous with occurrence of both illite-rich I/S ML (at 3492 m MD) with a FWHM higher than 0.4 °2θ and PCI (at 3582 m MD) with a FWHM close to 0.4 °2θ associated with micas/WCI in the fine fraction. This third zone is also characterized by the occurrence of chlorite.

Some supplementary mineralogical analyses are needed to differentiate propylitic chlorite resulting from the alteration of the primary biotite during the cooling of the granitic pluton, from potential ferrous chlorite which could occur in the FZs, as a result of the hydrothermal alteration of the granite (Vidal et al., 2018b).

If we focus on the permeable FZs intersected by the well at 3080, 3225 and 3365 m MD evidenced by T anomalies, different clay properties from the XRD results associated to these T anomalies are observed.

- **T-anomaly at 3050-3090 m MD**. From 3000 to 3100 m MD, the XRDs associated to the T anomaly evidence illitic material characterized by the systematic occurrence of illite-rich I/S ML. This is conveyed by high values of FWHM up to 0.6 °2θ.
- **T-anomaly at 3210-3230 m MD**. From 3210 to 3230 m MD, the XRDs associated to the T anomaly evidence illitic material composed of WCI (FWHM up to 0.3 °2θ) associated with primary micas (FWHM close to 0.15 °2θ).

- **T-anomaly at 3330-3390 m MD**. From 3300 to 3360 m MD, the XRDs associated to the T anomaly are not presenting the same signature than the two precedents permeable FZs. The FWHM values at 10 Å are homogeneous and very low (0.15 °2θ). The variations the ratio I_{002}/I_{001} (for the <5µm fraction) and the occurrence of d_{060} at 1.49 Å suggest the persistence of both di- and trioctahedral micas. These observations could suggest that natural permeability takes also place in fractures cross-cutting low hydrothermally altered granite.

More generally, it is observed that the FWHM of the 10 Å peak at depths of T anomalies are systematically expressed by scattered values. This scattering reflects the presence of illitic material containing +/- illite-rich I/S ML which could indicate changes in the physico-chemical conditions and/or a pulsed system with several generations of clayey material. The presence of illite-rich I/S ML in agreement with the temperatures measured in the drill-hole (minimum 155°C) are probably reflecting the latest stage of argilization related to fluid circulation in the fracture system.

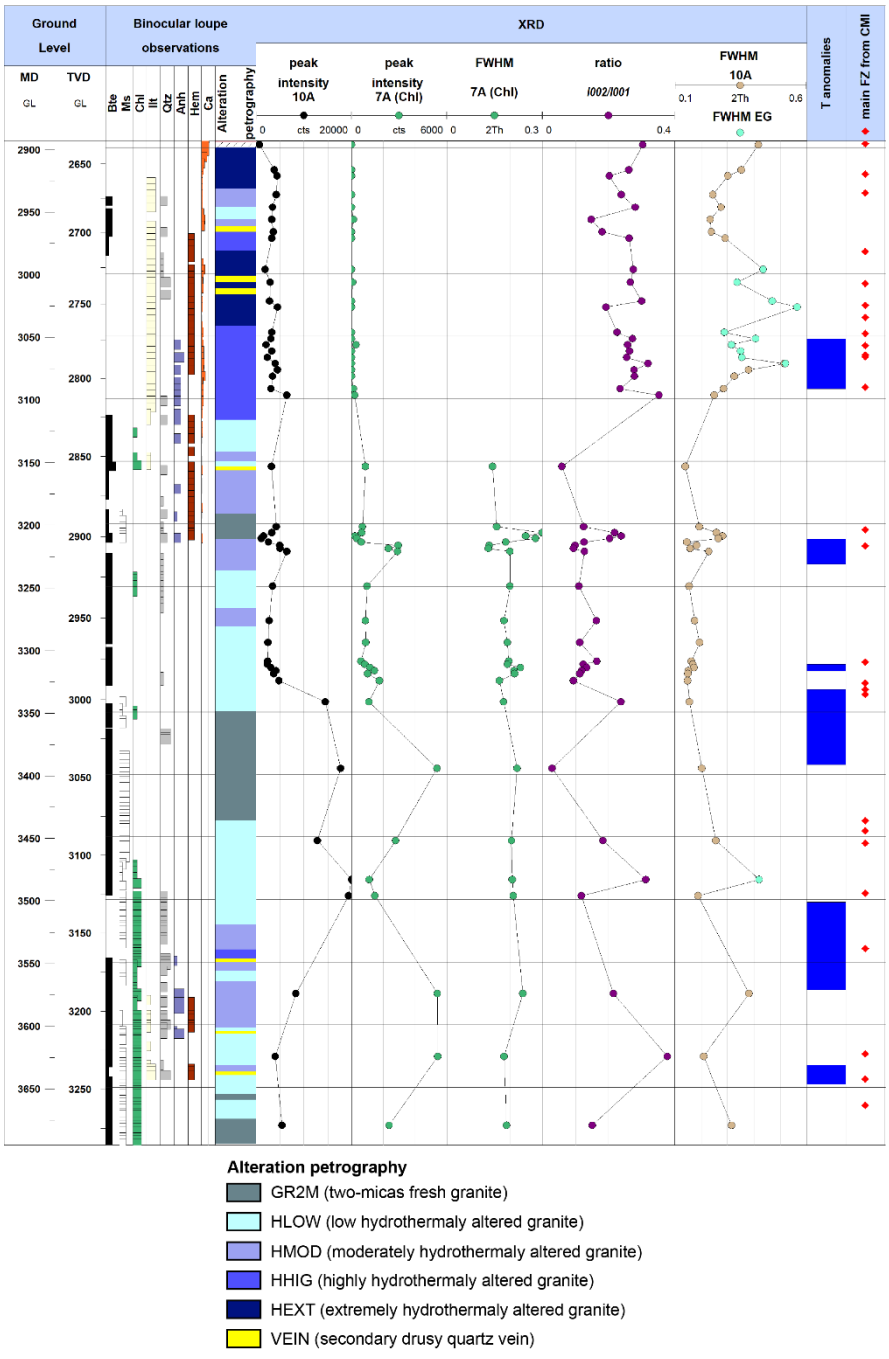

Figure 5: Composite log from GIL-1 presenting from left to right the alteration mineralogy and the alteration petrography from binocular loupe observation, the XRD results from the oriented fractions < 5 µm, ratios 060/001 and 002/001 are related to the 001 peak at 10 Å and the ratio 060/001 is from disoriented bulk powders. Blue dots in the FWHM at 10 Å are underlying the samples where a shift between the AD and EG diffractogramms was observed. T anomalies are from thermal logs realized post injection, in dark blue intense and in light blue less intense T anomalies. Main conductive fractures in red dots (right) were observed on the electrical image logs.

4.3 FZs derived from image logs in GIL-1

About 30 main conductive fractures have been analyzed from electrical image logs in GIL-1. They are not regularly distributed over the well but they are mainly concentrated between 2900-3100 m MD, around 3200 m MD, around 3350 m MD and deeper than 3450 m MD but with a more sparse distribution (Figure 6). T anomalies are located at 3051-3090, 3210-3230, 3330-3390, 3500-3570, and 3630-3645 m MD (Figure 6). These T anomalies systematically correlate with the conductive fractures visible (Figure 6). Surprisingly, all the conductive fractures visible on the electrical image logs do not present T anomalies. This could be explained by the fact that fractures appearing as conductive on both static and dynamic images could be due to the presence of conductive clay minerals which will tend to seal the fracture. For example, the conductive electrical fractures located from the top basement to 3050 m MD, do not match spatially with T log anomalies as well as those located around 3450 m MD (Figure 6).

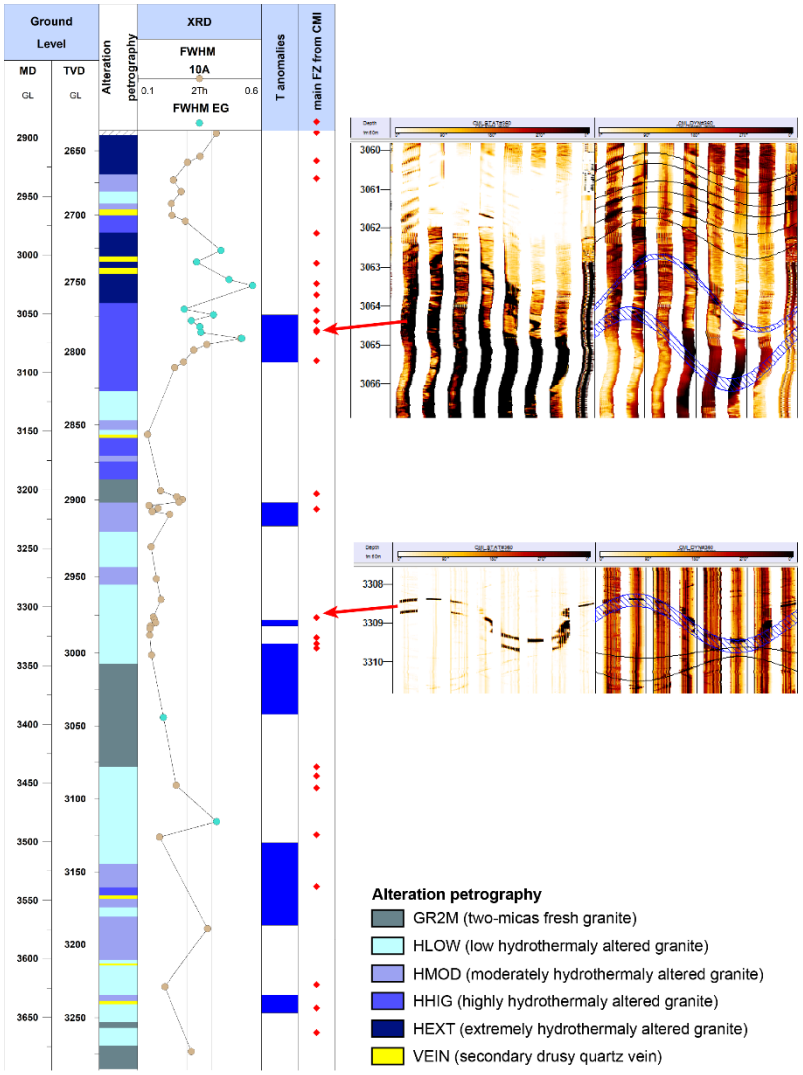

Figure 6: Composite log of the GIL-1 well presenting the alteration petrography, the FWHM of the 10 Å peak where blue dots in the FWHM at 10 Å are underlying the samples where a shift between the AD and EG diffractogramms was observed. T anomalies are from thermal logs realized post injection, in dark blue intense and in light blue less intense T anomalies. Main conductive fractures in red dots (right) were observed on the electrical image logs. Two electrical image show conductive fractures associated to the T anomalies.

5. DISCUSSION

In the granitic part of the GIL-1 well, two main stages of hydrothermal alteration were observed. Outside the FZs, propylitic alteration which corresponds to the cooling of the granitic pluton is observed and characterized by the occurrence of secondary chlorite +/- WCI. This paragenetic association needs to be confirmed by further petrographic observations, nevertheless it is quite common in the Soultz and Rittershoffen granite. This first alteration stage is superimposed by alteration parageneses linked to the fracture network. The most symptomatic secondary minerals associated with permeable reservoirs seem to be located between 2900 and 3100 m MD, where permeable FZs are characterized by PCI and illite-rich I/S ML which display scattered and high values of the 10 Å FWHM. The occurrence of both illite and illite-rich I/S ML traduces changes in the physico-chemical conditions of crystallization. This could be explained by crystallization kinetics linked to variable oversaturation of the fluids, changes in water-rock ratio, or pulsed fluids. The structure of FZs described in Soultz and Rittershoffen wells seems to be encountered in the Illkirch GIL-1 well as well, systematically characterized by secondary drusy quartz in the core zone and clay minerals like illite in the surrounding damage zone. The electrical image logs present a highly fractured granitic basement with a major conductive fracture located at the contact between the sedimentary cover and the granite. Image logs show a dense small-scale fracture network which could present a potential contribution to permeability, especially in the lowest part of the well from 3200 to 3700 m MD.

Conductive fractures are not always associated to T anomalies thus are not always permeable. Temperature signature in GIL-1 must be interpreted more in-depth and carefully until a temperature log at thermal equilibrium is acquired. The limits of the electrical image logs in terms of permeability interpretation also need to be considered. This rich structural dataset needs to be further investigated.

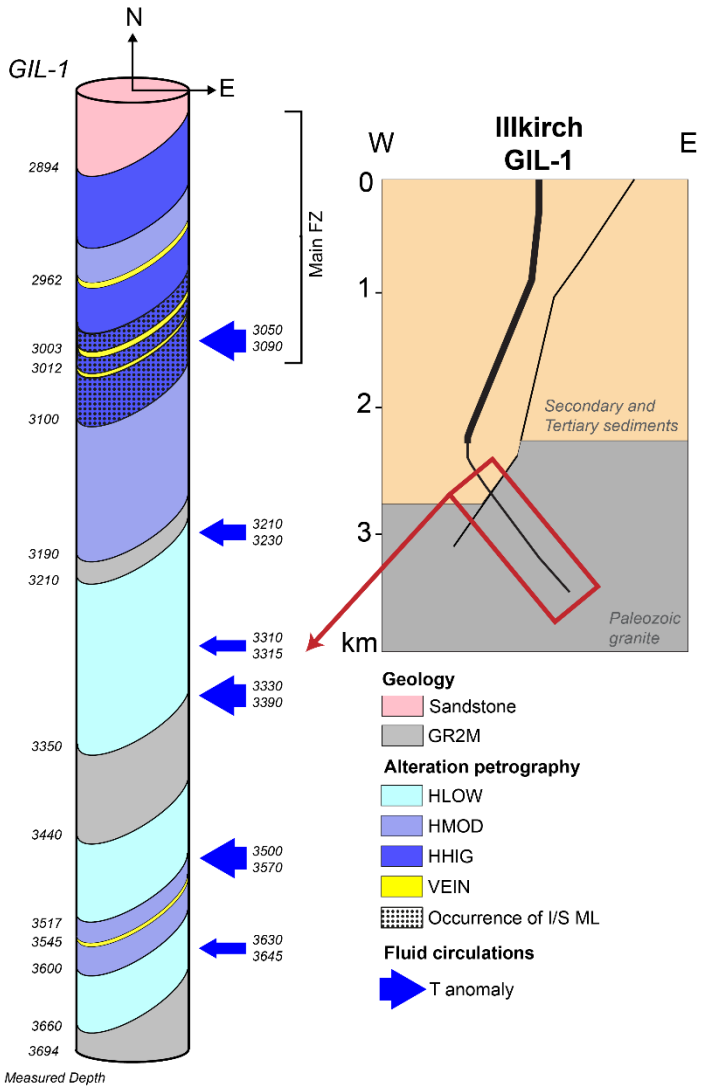

Figure 7: Conceptual model of hydrothermal alteration from the clay minerals along the granitic open-hole of GIL-1 well.

6. CONCLUSION

The combination of these methods helps to identify the hydrothermal alteration halos associated to the several temperature anomalies in a newly drilled geothermal well in the Strasbourg area. The binocular loupe observation enables to have a global description of the alteration granite facies in the well, as well as a qualitative petrographic description. The XRD method enables to have a qualitative description of 48 samples in the well to describe the clay signature of the alteration facies observed with the binocular loupe, but also of permeable FZs observed on the T log. In GIL-1, the most permeable structure seems to be located between 2900 and 3100 m MD. The upper part of the well (2900-3100 m MD) is characterized by the occurrence of clay minerals related to vein alteration (PCI, I/S ML). The HLOW zone from 3100-3350 m MD is characterized by the occurrences of clay minerals related to propylitic alteration (chlorite, +/- WCI). The downiest part seems more complex with alternation of HLOW to HHIG associated with the presence of polyphasic illitic material. The clay mineralogy of this zone needs to be further investigated by considering the structural data from electrical image logs.

The next step will be the quantification of the illitisation linked to the fluid circulation in the fracture network. That for, complementary investigations of the clay minerals will be done based on the SWIR data acquired in GIL-1. In Soultz and Rittershoffen wells, this method allowed identifying the alteration halo around the major permeable FZs and gave quantitative information about the illitic material quantity. In the URG granitic context, SWIR spectroscopy is an efficient method to quantify the alteration, once it has been calibrated with other mineralogical analyses like XRD as experienced at Soultz and Rittershoffen. In the Illkirch GIL-1 well, SWIR were acquired on the 250 cuttings samples of the granitic section and their interpretation will be done applying the methodology already used in Soultz and Rittershoffen wells.

The well GIL-1 intersected a dense fracture network composed of major conductive fractures observed on electrical image logs but also clusters of a small-scale conductive fracture network. Investigations of this fracture network are at the preliminary stage and will be deepened in the future in order to better conceptualize the model of circulations at the borehole scale.

ACKNOWLEDGMENTS

This work was realized in the framework of the PhD of Carole Glaas which is jointly supported by the ANRT (French Agency for Research and Technology) and ES-Géothermie. The authors acknowledge the EGS Alsace project co-funded by ADEME (French Agency for Environment) and ES SA, as well as ESIG, GEIE EMC, ECOGI for providing geoscientific data for Illkirch, Soultz and Rittershoffen respectively.

REFERENCES

Baillieux, P., Schill, E., Edel, J.-B., Mauri, G., 2013. Localization of temperature anomalies in the Upper Rhine Graben: insights from geophysics and neotectonic activity. International Geology Review 55, 1744–1762. https://doi.org/10.1080/00206814.2013.794914

Barton, C.A., Zoback, M.D., Moos, D., 1995. Fluid flow along potentially active faults in crystalline rock. Geology 23, 683–686. https://doi.org/10.1130/0091-7613(1995)023<0683:FFAPAF>2.3.CO;2

Baujard, C., Genter, A., Cuenot, N., Mouchot, J., Maurer, V., Hehn, R., Ravier, G., Seibel, O., Vidal, J., 2018. Experience from a successful soft stimulation and operational feedback after 2 years of geothermal power and heat production in Rittershoffen and Soultz-sous-Forêts plants (Alsace, France). Presented at the Geothermal Resource Council, Reno, Nevada, USA, pp. 2241–2252.

Baujard, C., Genter, A., Dalmais, E., Maurer, V., Hehn, R., Rosillette, R., Vidal, J., Schmittbuhl, J., 2017. Hydrothermal characterization of wells GRT-1 and GRT-2 in Rittershoffen, France: Implications on the understanding of natural flow systems in the Rhine Graben. 65, 255–268pp. https://doi.org/10.1016/j.geothermics.2016.11.001

Bradford, J., McLennan, J., Moore, J., Glasby, D., Waters, D., Kruwells, R., Bailey, A., Rickard, W., Bloomfield, K., King, D., 2013. Recent developments at the Raft River geothermal field. Presented at the Thirty-Eighth Workshop on Geothermal Reservoir Engineering, Stanford University, California, USA.

Brindley, G.W., Brown, G., 1980. Crystal Structures of Clay Minerals and their X-Ray Identification, Mineralogical Society of Great Britain and Ireland.

Cocherie, A., Guerrot, C., Fanning, C.M., Genter, A., 2004. Datation U–Pb des deux faciès du granite de Soultz (Fossé rhénan, France). Comptes Rendus Geoscience 336, 775–787pp. https://doi.org/10.1016/j.crte.2004.01.009

Davatzes, N.C., Hickman, S.H., 2005. Controls on fault-hosted fluid flow; Preliminary results from the Coso Geothermal Field, CA. Presented at the Geothermal Resources Council Transactions, Geothermal Resources Council, Davis, California, pp. 343–348.

Dezayes, C., Genter, A., Valley, B., 2010. Structure of the low permeable naturally fractured geothermal reservoir at Soultz. C. R. Geoscience 342, 517–530. https://doi.org/10.1016/j.crte.2009.10.002

Dezayes, C., Lerouge, C., 2019. Reconstructing Paleofluid Circulation at the Hercynian Basement/Mesozoic Sedimentary Cover Interface in the Upper Rhine Graben. Geofluids 2019, 1–30. https://doi.org/10.1155/2019/4849860

Edel, J.B., Maurer, V., Dalmais, E., Genter, A., Richard, A., Letourneau, O., Hehn, R., 2018. Structure and nature of the Palaeozoic basement based on magnetic, gravimetric and seismic investigations in the central Upper Rhinegraben: Focus on the deep geothermal project of Illkirch-Graffenstaden. Geothermal Energy 6. https://doi.org/10.1186/s40517-018-0099-y

Garnish, J.D., 1985. Hot Dry Rock - A European perspective. GRC Hawaï.

Genter, A., Evans, K., Cuenot, N., Fritsch, D., Sanjuan, B., 2010. Contribution of the exploration of deep crystalline fractured reservoir of Soultz to the knowledge of enhanced geothermal systems (EGS). Comptes Rendus Geoscience 342, 502–516. https://doi.org/10.1016/j.crte.2010.01.006

Genter, A., Traineau, H., 1996. Analysis of macroscopic fractures in granite in the HDR geothermal well EPS-l, Soultz-sous-Forets, France. Journal of Volcanology and Geothermal Research 121–141.

Genter, A., Traineau, H., Artignan, D., 1997. Synthesis of geological and geophysical data at Soultz-sous-Forêts (France) (No. 39440). BRGM, Orléans, France.

Genter, A., Traineau, H., Dezayes, C., Elsass, P., Ledésert, B., Meunier, A., Villemin, T., 1995. Fracture Analysis and Reservoir Characterization of the Granitic Basement in the HDR Soultz Project (France). Geotherm. Sci. & Tech. 4, 189–214.

Genter, A., Traineau, H., Ledésert, B., Bourgine, B., Gentier, S., 2000. Over 10 years of geological investigations within the HDR Soultz project, France. Presented at the World Geothermal Congress, Kyushu, Japan, pp. 3707–3712.

GeOrg, T., 2017. EU-Projekt GeORG - Geoportal [WWW Document]. URL http://www.geopotenziale.org/home?lang=3

Gérard, A., Kappelmeyer, O., 1987. The Soultz-sous-Forêts project. Geothermics 16, 393–399.

Gérard, A., Menjoz, A., Schwoerer, P., 1984. L'anomalie thermique de Soultz-sous-Forêts. Géothermie Actualités 35–42.

Glaas, C., Genter, A., Girard, J.F., Patrier, P., Vidal, J., 2018. How do the geological and geophysical signatures of permeable fractures in granitic basement evolve after long periods of natural circulation? Insights from the Rittershoffen geothermal wells (France). Geothermal Energy 6. https://doi.org/10.1186/s40517-018-0100-9

Glaas, C., Vidal, J., Patrier, P., Beaufort, D., Genter, A., 2019. Contribution of SWIR to the Clay Signature of Permeable Fracture Zones in the Granitic Basement. Overview of Soultz and Rittershoffen wells. Presented at the European Geothermal Congress, Den Haag, The Netherlands, 11-14 June, p. 11.

Hébert, B., 2018. Approche quantitative par spectrométrie Vis-NIR des minéraux argileux et uranifères dans les sables du gisement de Tortkuduk, Kazakhstan. Université de Poitiers, Poitiers.

Hébert, R.L., Ledésert, B., Bartier, D., Dezayes, C., Genter, A., Grall, C., 2010. The Enhanced Geothermal System of Soultz-sous-Forêts: A study of the relationships between fracture zones and calcite content. Journal of Volcanology and Geothermal Research 196, 126–133. https://doi.org/10.1016/j.jvolgeores.2010.07.001

Hunt, G.L., Salisbury, J.W., 1970. Visible and Near Infrared Spectra of Minerals and Rocks: I. Silictae Minerals. Modern Geology 1, 283–300.

Jacquemont, B., 2002. Etude des interactions eaux-roches dans le granite de Soultz-sous-Forêts. Quantification et modélisation des transferts de matière par les fluides. (PhD). Université de Strasbourg, France.

Kappelmeyer, O., 1991. European HDR project at Soultz-sous-Forêts general presentation. Geotherm. Sci. & Tech. 263–289.

Ledésert, B., Berger, G., Meunier, A., Genter, A., Bouchet, A., 1999. Diagenetic-type reactions related to hydrothermal alteration in the Soultz-sous-Forets Granite, France. European Journal of Mineralogy 11, 731–741.

Ledésert, B., Hebert, R., Genter, A., Bartier, D., Clauer, N., Grall, C., 2010. Fractures, hydrothermal alterations and permeability in the Soultz Enhanced Geothermal System. Comptes Rendus Geoscience 342, 607–615. https://doi.org/10.1016/j.crte.2009.09.011

Ledésert, B., Hébert, R.L., Grall, C., Genter, A., Dezayes, C., Bartier, D., Gérard, A., 2009. Calcimetry as a useful tool for a better knowledge of flow pathways in the Soultz-sous-Forêts Enhanced Geothermal System. Journal of Volcanology and Geothermal Research 181, 106–114. https://doi.org/10.1016/j.jvolgeores.2009.01.001

Madejová, J., Gates, W.P., Petit, S., 2017. IR Spectra of Clay Minerals, in: Developments in Clay Science. Elsevier, pp. 107–149. https://doi.org/10.1016/B978-0-08-100355-8.00005-9

Mas, A., Guisseau, D., Patrier, P., Beaufort, D., Sanjuan, B., Girard, J.P., 2006. Clay minerals related to the hydrothermal activity of the Bouillante geothermal field (Guadeloupe). Journal of Volcanology and Geothermal Research 158, 380–400.

Meller, C., Genter, A., Kohl, T., 2014. The application of a neural network to map clay zones in crystalline rock. Geophysical Journal International 196, 837–849. https://doi.org/10.1093/gji/ggt423

Meller, C., Kohl, T., 2014. The significance of hydrothermal alteration zones for the mechanical behavior of a geothermal reservoir. Geothermal Energy 2. https://doi.org/10.1186/s40517-014-0012-2

Meller, C., Ledésert, B., 2017. Is There a Link Between Mineralogy, Petrophysics, and the Hydraulic and Seismic Behaviors of the Soultz-sous-Forêts Granite During Stimulation? A Review and Reinterpretation of Petro-Hydromechanical Data Toward a Better Understanding of Induced Seismicity and Fluid Flow. Journal of Geophysical Research: Solid Earth 122, 9755–9774. https://doi.org/10.1002/2017JB014648

Moore, D.M., Reynolds, R.C., 1997. X-Ray Diffraction and the Identification and Analysis of Clay Minerals.

Nishimoto, S., Yoshida, H., 2010. Hydrothermal alteration of deep fractured granite: Effects of dissolution and precipitation. Lithos 115, 153–162. https://doi.org/10.1016/j.lithos.2009.11.015

Patrier, P., Papapanagiotou, P., Beaufort, D., Traineau, H., Bril, H., Rojas, J., 1996. Role of permeability versus temperature in the distribution of the fine (< 0.2 μm) clay fraction in the Chipilapa geothermal system (El Salvador, Central America). Journal of Volcanology and Geothermal Research 72, 101–120. https://doi.org/10.1016/0377-0273(95)00078-X

Pontual, S., Merry, N., Gamson, P., 1997. G-Mex Vol.1, Spectral interpretation field manual. Ausspec international Pty. Ltd., Kew, Victoria 3101, Australia.

Richard, A., Maurer, V., Edel, J.-B., Genter, A., Baujard, C., Dalmais, E., 2016. Towards targeting geothermal reservoir: exploration program for a new EGS project in urban context in Alsace, in: European Geothermal Congress. Strasbourg, France.

Sausse, J., Fourar, M., Genter, A., 2006. Permeability and alteration within the Soultz granite inferred from geophysical and flow log analysis. Geothermics 544–560.

Sausse, J., Genter, A., 2005. Types of permeable fractures in granite. Geological Society, London, Special Publications 240, 1–14. https://doi.org/10.1144/GSL.SP.2005.240.01.01

Schellschmidt, R., Clauser, 1996. The thermal regime of the upper rhine graben and the anomaly at Soultz. Z. Angew. Geologie 42, 40–44.

Schumacher, M.E., 2002. Upper Rhine Graben: Role of preexisting structures during rift evolution. Tectonics 21, 6-1-6–17. https://doi.org/10.1029/2001TC900022

Smith, M.P., Savary, V., Yardley, B.W.D., Valley, J.W., Royer, J.J., Dubois, M., 1998. The evolution of the deep flow regime at Soultz-sous-Forêts, Rhine Graben, eastern France: Evidence from a composite quartz vein. Journal of Geophysical Research: Solid Earth 103, 27223–27237.

Stussi, J.-M., Cheilletz, A., Royer, J.-J., Chèvremont, P., Féraud, G., 2002. The hidden monzogranite of Soultz-sous-Forêts (Rhine Graben, France). Mineralogy, petrology and genesis. Géologie de la France 45–64.

Traineau, H., Genter, A., Cautru, J.-P., Fabriol, H., Chèvremont, Ph., 1992. Petrography of the granite massif from drill cutting analysis and well log interpretation in the geothermal HDR borehole GPK-1 (Soultz, Alsace, France), in: Geothermal Energy in Europe - The Soultz Hot Dry Rock Project. Bresee, James C., Montreux, Switzerland, pp. 1–29.

Vidal, J., Genter, A., 2018. Overview of naturally permeable fractured reservoirs in the central and southern Upper Rhine Graben: Insights from geothermal wells. Geothermics 74, 57–73. https://doi.org/10.1016/j.geothermics.2018.02.003

Vidal, J., Glaas, C., Hébert, B., Patrier, P., Beaufort, D., 2018a. Use of SWIR spectroscopy for the exploration of permeable fracture zones in geothermal wells at Rittershoffen (Alsace, France). Presented at the Geothermal Resources Council, Reno, USA, p. 10.

Vidal, J., Hehn, R., Glaas, C., Genter, A., 2019. How can temperature logs help identify permeable fractures and define a conceptual model of fluid circulation? An example from deep geothermal wells in the Upper Rhine Graben. Geofluids 14. https://doi.org/10.1155/2019/3978364

Vidal, J., Patrier, P., Genter, A., Beaufort, D., Dezayes, C., Glaas, C., Lerouge, C., Sanjuan, B., 2018b. Clay minerals related to the circulation of geothermal fluids in boreholes at Rittershoffen (Alsace, France). Journal of Volcanology and Geothermal Research 349, 192–204. https://doi.org/10.1016/j.jvolgeores.2017.10.019

Villemin, T., Bergerat, F., 1987. L'évolution structurale du fossé rhénan au cours du Cénozoïque : un bilan de la déformation et des effets thermiques de l'extension. Bull. Soc. géol. France 8, 245–255.